Chapter 1

Mass Density and Saturation

"The central nuclear charge density is nearly the same for all nuclei. Nucleons do not congregate near the center."

K. S. Krane

1.1 From charge density to mass density

Electron scattering maps the proton (charge) density $\rho_p(r)$. A central empirical fact is that this density is nearly the same in the interior of all nuclei: nucleons do not pile up at the centre. Empirically one fits

$$\rho_p(r) = \frac{\rho_p(0)}{1 + \exp\big[(r - R)/a\big]}, \tag{1.1}$$

with a nearly universal surface diffuseness $a = 0.52\,\mathrm{fm} \pm 0.01\,\mathrm{fm}$ and a half-density radius $R_0 = 1.2\,\mathrm{fm} \times A^{1/3}$ [1, 6].

Electrons do not couple to neutrons. The full nucleon density, often called the mass or matter density, must be reconstructed from the charge density together with a model of how neutrons are distributed, or measured with hadronic probes. That matter density, and the near constancy of its central value, is the subject of this chapter. It is also the microscopic reason the strong force must be short ranged: if every nucleon attracted every other nucleon, neither the density nor the binding energy would scale as they do [6].

Here $\rho_p(r)$ denotes the *proton number density* (nucleons per fm^3), not the electromagnetic charge density $e\,\rho_p$. Electron scattering determines ρ_p because the charge density is $e\,\rho_p$ for point-like protons (up to small meson-exchange corrections). It is equally important to know the distribution of *all* nucleons (neutrons and protons), because nuclear binding, the equation of state, and the liquid-drop model all refer to the total nucleon number density $\rho(r)$. (The true mass density is $m_N\rho$; nuclear physics usually quotes number densities.)

Since neutrons are uncharged, ordinary Coulomb scattering does not observe them. Under a standard working assumption, however, one can still infer $\rho(r)$ from $\rho_p(r)$.

1.1.1 The constant N/Z assumption

A nucleus with N neutrons and Z protons has overall ratio N/Z and mass number $A = N + Z$. It is usually assumed that the local neutron-to- proton density ratio is the same everywhere inside the nucleus:

$$\frac{\rho_n(r)}{\rho_p(r)} = \frac{N}{Z}. \tag{1.2}$$

The total nucleon density is the sum

$$\rho(r) = \rho_n(r) + \rho_p(r). \tag{1.3}$$

Eliminating ρ_n between these two equations gives immediately

$$\rho(r) = \rho_p(r)\left(1 + \frac{N}{Z}\right) = \rho_p(r)\,\frac{A}{Z}. \tag{1.4}$$

Definition: nucleon (mass) density from charge density

Under the assumption $\rho_n/\rho_p = N/Z$ everywhere,

$$\rho(r) = \frac{A}{Z}\,\rho_p(r).$$

Rescaling the measured proton density by A/Z converts a charge distribution into an estimate of the total nucleon density.

Caution

Equation (1.2) is an approximation, not a theorem. In heavy nuclei ($N > Z$) a *neutron skin* develops: $\rho_n(r)$ extends farther than $\rho_p(r)$. The constant-ratio assumption then fails in the surface. For the bulk and for light or near-symmetric nuclei it remains a useful first estimate; for precision neutron-skin physics one needs parity-violating electron scattering or hadronic probes (cf. Lecture 1).

1.1.2 What the rescaled densities look like

Figure 1.1 recalls the proton densities of ^{16}O, ^{118}Sn, and ^{197}Au. Applying Equation (1.4) produces the nucleon densities of Figure 1.2. Two features stand out at once.

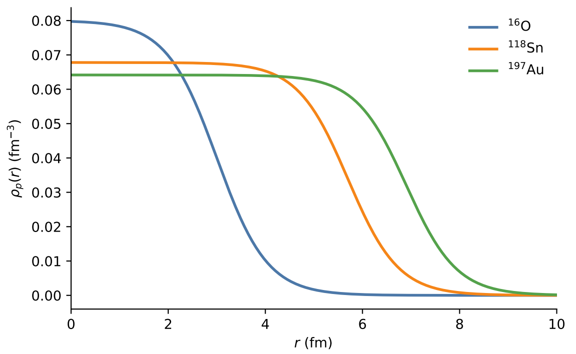

Figure 1.1: Proton densities $\rho_p(r)$ for ^{16}O, ^{118}Sn, and ^{197}Au.

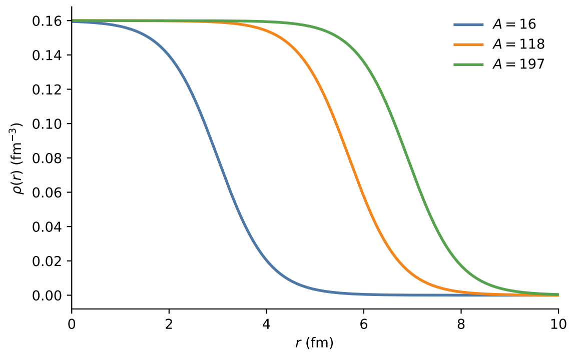

Figure 1.2: Nucleon densities $\rho = (A/Z)\rho_p$ with common central ρ_0.

1. The half-density radii and surface widths are essentially the same as in the charge densities:

rescaling multiplies the vertical axis, not the radial shape.

2. All three nuclei now share virtually the *same central nucleon density*, $\rho_0 \approx 0.16--0.17\,1/\mathrm{fm}^3$.

Key idea

Saturation of nuclear matter: the central nucleon density is nearly independent of mass number [1]. Nuclei are not denser in the middle when they grow larger; they grow by adding a larger volume at fixed bulk density. Together with $B/A \approx$ constant, this strongly supports a saturating, short-range effective interaction. Density systematics alone do not prove a particular microscopic force: Pauli pressure, short-range repulsion, tensor correlations, and many-body forces all participate in setting the saturation point.

1.2 Woods–Saxon parameters and the nuclear surface

The nucleon density is again described by a Woods–Saxon (two-parameter Fermi) profile,

$$\rho(r) = \frac{\rho_0}{1 + \exp\left[(r-R)/a\right]}, \tag{1.5}$$

where now ρ_0 is the central *nucleon* density, R is the half-density radius, and a is the diffuseness.

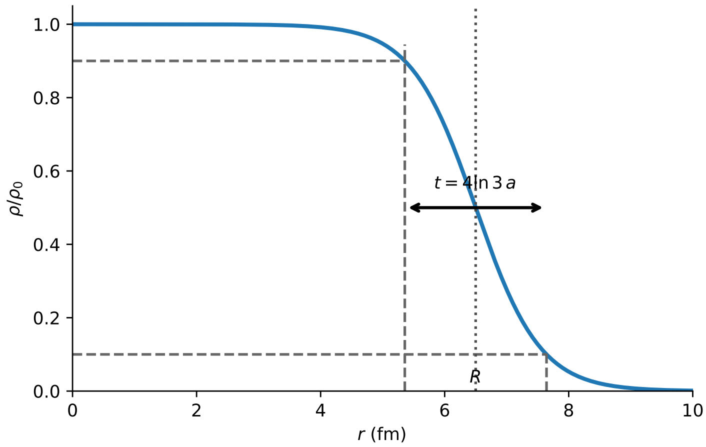

Figure 1.3: Geometry of the Woods–Saxon surface. The half-density radius R is the point where $\rho = \rho_0/2$. The surface thickness t, from $0.9\rho_0$ to $0.1\rho_0$, equals $4a \ln 3 \approx 4.4\,a$.

1.2.1 Surface thickness from first principles

To relate a to an observable surface thickness, evaluate the radii at which the density has fallen to 90% and 10% of ρ_0.

Setting $\rho = 0.9\rho_0$,

$$0.9\rho_0 = \frac{\rho_0}{1 + e^{(r-R)/a}} \implies e^{(r-R)/a} = \frac{1}{9} \implies \frac{r-R}{a} = -\ln 9 = -2\ln 3. \tag{1.6}$$

Hence

$$r_{90} = R - a\ln 9 = R - 2a\ln 3 \approx R - 2.20\,a. \tag{1.7}$$

Setting $\rho = 0.1\rho_0$,

$$0.1\rho_0 = \frac{\rho_0}{1+e^{(r-R)/a}} \implies e^{(r-R)/a} = 9 \implies r_{10} = R + 2a\ln 3 \approx R + 2.20\,a. \tag{1.8}$$

The surface thickness is therefore

$$t \equiv r_{10} - r_{90} = 4a\ln 3 \approx 4.39\,a. \tag{1.9}$$

Remark

Lecture notes sometimes quote $t \approx 4.6a$ by approximating $\ln 9 \approx 2.3$. The exact factor is $4\ln 3 \approx 4.394$. A standard global fit gives $a = 0.52\,\text{fm} \pm 0.01\,\text{fm}$ [1], so

$$t = 4a\ln 3 \approx 4.39 \times 0.52\,\text{fm} \approx 2.28\,\text{fm}.$$

The nuclear "skin" is only a couple of fermis thick and is nearly independent of A. The redrawn Figure 1.3 uses the exact label $4\ln 3\,a$, so figure and derivation now follow the same convention.

Example: surface of a heavy nucleus

With $a = 0.52\,\text{fm}$,

$$t \approx 2.3\,\text{fm}.$$

For ^{197}Au, $R_0 = 1.2\,\text{fm} \times 197^{1/3} \approx 7.0\,\text{fm}$ [1]. The density is essentially flat for $r \lesssim 5\,\text{fm}$ and has fallen to a few percent of ρ_0 by $r \approx 9 - -10\,\text{fm}$, matching Figure 1.2.

The central core is uniformly populated with nucleons up to $r \sim R$; beyond that the density decreases smoothly. The nucleus does not have a sharp boundary but a diffuse quantum surface.

1.2.2 The $A^{1/3}$ law for the half-density radius

The mean nuclear radius R_0 increases with mass number. Saturation already implies the functional form. If the central density is A-independent, the volume that holds A nucleons must grow as

$$A = \tfrac{4}{3}\pi R^3\,\rho_0 \quad\Rightarrow\quad R = \left(\frac{3}{4\pi\rho_0}\right)^{1/3} A^{1/3} \equiv r_0\,A^{1/3}. \tag{1.10}$$

With $\rho_0 \approx 0.16\,\text{fm}^{-3}$,

$$r_0 = \left(\frac{3}{4\pi \times 0.16}\right)^{1/3} \approx 1.14\,\text{fm}, \tag{1.11}$$

close to the conventional fit value. This 1.14 fm is the radius of a sharp uniform sphere whose *mean* density is $0.16\,\text{fm}^{-3}$; it is not numerically identical to a Woods–Saxon half-density radius, an rms radius, or a charge radius. Surface diffuseness and the chosen radius definition account for the familiar $r_0 \simeq 1.2\,\text{fm}$ convention. Analysis of electron-scattering data yields the empirical expression [1]

$$R_0 = 1.2\,\text{fm} \times A^{1/3}. \tag{1.12}$$

Combined with a constant central density, this is precisely the geometry of an incompressible liquid drop: volume $\propto A$, so radius $\propto A^{1/3}$. Equation (1.12) is a standard input to the liquid-drop model [1].

The mean inter-nucleon spacing at saturation follows from the same density:

$$d \sim \rho_0^{-1/3} \approx (0.16)^{-1/3}\,\mathrm{fm} \approx 1.8\,\mathrm{fm}, \tag{1.13}$$

comparable to the pion Compton wavelength that will appear in Lecture 11.

Takeaway

Three numbers characterise bulk nuclear matter as seen by electrons (rescaled to nucleons) [1]:

$$\rho_0 \approx 0.16/\mathrm{fm}^3, \quad R_0 = 1.2\,\mathrm{fm}\,A^{1/3}, \quad a = 0.52\,\mathrm{fm} \pm 0.01\,\mathrm{fm} \ \ (t \approx 2.3\,\mathrm{fm}).$$

They will reappear in the liquid-drop model, the semi-empirical mass formula, and the nuclear equation of state.

1.3 What uniform density teaches about the strong force

The nucleus exists because a strong attractive force counters the Coulomb repulsion among protons. Without that force the nucleus would explode. Nuclear attraction is far stronger than Coulomb repulsion at fermi distances, yet the density profile is *flat*, not centrally peaked.

One might have expected the opposite. In a self-gravitating body such as the Earth, density is highest at the core and decreases toward the surface: every mass element attracts every other, so the equilibrium is centrally condensed. Why is the nucleus different?

Key idea

Nuclear forces are *short-ranged.* A given nucleon interacts significantly only with its nearest neighbours, not with all other nucleons in the system. There is therefore no long-range "pull toward the centre," and the equilibrium density is set locally by the balance of short-range attraction and short-range repulsion (the hard core / Pauli pressure). The result is a saturated, roughly constant bulk density.

Remark

The range of the strong force is of order the pion Compton wavelength, $\hbar/(m_\pi c) \approx 1.4\,\mathrm{fm}$—comparable to the mean inter-nucleon spacing at saturation. Beyond two or three fermis the force has essentially died away. That is why adding nucleons increases the *volume* at fixed density rather than packing the centre more tightly, and why the surface thickness is a nearly universal few fermis set by the force range itself.

Historical note: Hideki Yukawa (1907–1981)

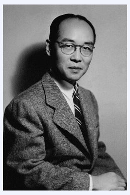

Hideki Yukawa, working in Osaka in 1934–1935, proposed that the short-range nuclear force is mediated by the exchange of a massive boson. The resulting potential,

$$V(r) \propto \frac{e^{-r/\lambda}}{r}, \qquad \lambda = \frac{\hbar}{mc},$$

falls exponentially with a range fixed by the mediator mass m. Yukawa estimated $m \sim 100\,\mathrm{MeV}/c^2$; the pion, discovered in 1947, has $m_\pi \approx 140\,\mathrm{MeV}/c^2$ and $\lambda \approx 1.4\,\mathrm{fm}$. He received the 1949 Nobel Prize in Physics, the first Nobel awarded to a Japanese scientist. Yukawa's insight is the microscopic reason the nuclear density saturates: the force simply does not reach across the whole nucleus.

1.4 Preview: finite-size spectroscopy

Electron scattering is not the only radius probe. For an atomic s state, the leading correction caused by replacing a point nucleus with a spherical charge distribution is

$$\Delta E_{ns} = \frac{2\pi}{3}\frac{Ze^2}{4\pi\varepsilon_0}\,|\psi_{ns}(0)|^2\langle r^2\rangle_{\mathrm{ch}} + \cdots . \tag{1.14}$$

The positive sign means that a finite nucleus softens the Coulomb singularity and raises the bound-state energy. This compact theorem, rather than a second uniform-sphere derivation, is all that is needed here. Lecture 3 derives it, reduces it to the uniform-sphere result $\langle r^2\rangle = 3R^2/5$, and explains how field shifts are separated from recoil (mass) shifts in real isotope spectroscopy.

1.5 Summary and outlook

- Electron scattering measures $\rho_p(r)$. Under $\rho_n/\rho_p = N/Z$, the nucleon density is $\rho = (A/Z)\,\rho_p$.
- Rescaled densities for different nuclei share a common central value $\rho_0 \approx 0.16/\mathrm{fm}^3$: nuclear matter saturates.
- The Woods–Saxon surface thickness is $t = 4a\ln 3$ with the usual $a = 0.52\,\mathrm{fm} \pm 0.01\,\mathrm{fm}$ ($t \approx 2.3\,\mathrm{fm}$); the half-density radius obeys $R_0 = 1.2\,\mathrm{fm}\,A^{1/3}$ [1].
- A flat bulk density is the geometric signature of a short-range strong force: nucleons feel only their neighbours.
- Atomic electrons (and especially muons) provide a second radius measurement via the finite-size shift $\Delta E \propto Z\,|\psi(0)|^2\,\langle r^2\rangle_{\mathrm{ch}}$.

Next. Lecture 3 specialises the finite-size shift to isotope differences and muonic atoms, recovering the same $R_0 \approx 1.2\,\mathrm{fm}$ from spectroscopy. Lectures 4–5 then leave size for binding energy and the SEMF that encodes saturation as a volume term.

1.6 Deeper physics: saturation density and short-range force

1.6.1 Numerical saturation density

If the mass density is roughly uniform inside $R = r_0 A^{1/3}$ with $r_0 \approx 1.2\,\mathrm{fm}$, the mean nucleon density is

$$\rho_0 = \frac{A}{\frac{4}{3}\pi R^3} = \frac{3}{4\pi r_0^3} \approx 0.14\text{–}0.17\,\mathrm{fm}^{-3}, \tag{1.15}$$

depending on the precise radius definition (half-density vs equivalent uniform sphere vs rms). A representative value is $\rho_0 \approx 0.16\,\mathrm{fm}^{-3}$ [1, 2, 4]. In mass units this is

$$\bar{\rho} \sim 2.3 \times 10^{17}\,\mathrm{kg\,m^{-3}} \sim 2 \times 10^{14}\,\mathrm{g\,cm^{-3}}, \tag{1.16}$$

about 10^{14} times liquid water: the densest stable bulk matter on Earth is ordinary nuclear matter.

1.6.2 Why density saturation implies a short-range force

If every nucleon interacted attractively with every other nucleon (infinite-range two-body force), the binding energy would grow as $\binom{A}{2} \propto A^2$ and the equilibrium density would not be A-independent. Observed $B \propto A$ (Lecture 4) and $\rho \approx$ const together require that each nucleon feels only a fixed number of neighbours: the force range is of order the internucleon spacing ~ 1–$2\,\mathrm{fm}$.

Light vs heavy surface fraction

With $t \approx 2.3\,\mathrm{fm}$ fixed and $R = 1.2\,A^{1/3}\,\mathrm{fm}$, a light nucleus ($R \sim 3\,\mathrm{fm}$) is mostly surface, while lead ($R \sim 7\,\mathrm{fm}$) is mostly bulk. That geometric fact foreshadows the SEMF: surface energy dominates the rise of B/A at low A; volume energy dominates the mid-mass plateau [1].

Remark

Mass vs charge distributions. Matter densities inferred from hadronic probes are similar in shape to charge densities, but not identical: neutron skins in heavy nuclei make the matter radius slightly larger than the charge radius. Lecture 1's electron probe measures charge; Lecture 2's saturation argument concerns the *matter* density that sets the SEMF volume term.

1.7 Physics depth: saturation density and force range

Lecture 2 established $\rho_0 \sim 0.16\,\mathrm{fm}^{-3}$ and $R \propto A^{1/3}$. Those two facts fix both a length and an energy scale for every later liquid-drop argument.

1.7.1 Worked estimate: Fermi momentum and kinetic scale

For a symmetric Fermi gas at density $n_0 = 0.16\,\mathrm{fm}^{-3}$,

$$k_F = (3\pi^2 n_0/2)^{1/3} \simeq 1.33\,\mathrm{fm}^{-1}, \qquad T_F = \frac{\hbar^2 k_F^2}{2m_N} \simeq 37\,\mathrm{MeV}. \tag{1.17}$$

The observed volume energy $\sim 16\,\mathrm{MeV}$ per nucleon then implies a potential contribution of order $-50\,\mathrm{MeV}$ per nucleon once kinetic energy is subtracted: attraction and Fermi motion nearly cancel. That cancellation is delicate; three-nucleon forces and the density dependence of the symmetry energy move the equilibrium point by only a few percent in n_0 but can change the pressure above saturation by much more (Lecture 6).

Internucleon spacing

The mean spacing $d \sim n_0^{-1/3} \simeq 1.8\,\mathrm{fm}$ is comparable to the pion Compton wavelength $\hbar/(m_\pi c) \simeq 1.4\,\mathrm{fm}$ (Lecture 11). Saturation therefore lives at the border between a long-range one-pion tail and a short-range repulsive core: neither a pointlike contact force nor an infinite-range $1/r$ force can produce an A-independent bulk density.

Remark

Assumptions. Uniform-density estimates ignore surface, Coulomb, and shell oscillations. They are excellent for order-of-magnitude pedagogy and poor as precision EOS inputs. Always state whether n_0 is a charge or matter density when comparing electron scattering with heavy-ion or astrophysical constraints.

1.7.2 Compressibility and the breathing mode

The incompressibility $K = 9n_0^2(\partial^2(E/A)/\partial n^2)_{n_0}$ sets the curvature of the energy per nucleon at saturation. Giant monopole resonance energies constrain $K \sim 220$–$260\,\mathrm{MeV}$ in symmetric matter. That number is the laboratory cousin of the speed of sound just above n_0. Soft EOS families with small K yield more compact stars at fixed mass; stiff families push radii outward. Quoting n_0 without K is like quoting a spring's equilibrium length without its spring constant.

Surface symmetry energy and the neutron-skin thickness further split isovector from isoscalar physics. A nucleus with a thick neutron skin looks like a laboratory droplet with an enhanced local asymmetry at the surface, connecting Lecture 1's radii to Lecture 2's saturation argument without yet invoking stars.

A Fermi-gas pressure $P = (2/5)nT_F$ at saturation is tens of mega-electronvolts per cubic femtometre, enormous on laboratory scales yet the baseline that gravity must overcome in Lecture 6. Adding interactions changes both the energy and the pressure; the slope of E/A versus n away from n_0 is the EOS. Students should plot a schematic E/A with a minimum at n_0 and mark K as curvature: that single sketch organises saturation, giant resonances, and neutron-star radii.

Pressure sketch

From a quadratic expansion of E/A about n_0, derive $P \approx (K/9)(n - n_0)^2/n_0$ near saturation (schematic) and discuss why $P(n_0) = 0$. This short derivation links Lecture 2 to the EOS language of Lecture 6 without solving TOV equations.

1.8 Further physics: saturation and the uncertainty principle

Constant central density and $B/A \sim$ const are two faces of the same fact: each nucleon interacts mainly with nearest neighbours (**saturation** of the nuclear force). A quantum link makes that plausible. If A nucleons share a volume $\propto R^3$ with $R = r_0 A^{1/3}$, each occupies a linear size $\Delta x \sim r_0$. The uncertainty principle then gives a mean kinetic energy per nucleon of order

$$\langle T \rangle \sim \frac{\hbar^2}{2m_N r_0^2} \sim \text{tens of MeV}, \tag{1.18}$$

nearly independent of A. Because the kinetic energy per particle does not grow with system size, neither does the net binding per nucleon once nearest-neighbour attraction is fixed [14].

That argument fails for atoms: the long-range Coulomb field of the nucleus pulls electrons tighter as Z grows, so atomic size does not scale as $Z^{1/3}$ and the electron density rises with Z. Nuclear forces do not act that way: density saturates.

1.8.1 Saturation requires more than the Pauli principle

Nearest-neighbour counting explains why density and B/A do not grow with A, but a complete picture of saturation needs three ingredients [14]:

1. short-range attraction ($r \sim 1\,\text{fm}$);
2. a repulsive "hard core" at $r \lesssim 0.5\,\text{fm}$ (partly Pauli/quark structure);
3. the Pauli principle for nucleons as fermions.

Any pure power-law attraction would not saturate. The empirical Woods–Saxon density (flat interior, thin surface) is the geometric fingerprint of that three-part force.

1.8.2 Atoms vs nuclei

Atomic size does *not* grow as $Z^{1/3}$: the long-range Coulomb field of the nucleus increases electron density with Z. Nuclear density is approximately constant because the force is short-ranged and saturates. That contrast is the essential reason liquid-drop thinking works for nuclei and not for atoms [14, 5].

1.8.3 Fermi momentum and density at saturation

Treat protons and neutrons as independent Fermi gases in a volume $V = (4\pi/3)R^3$ with bulk density

$$n_0 \approx 0.15\text{–}0.17\,\text{fm}^{-3} \tag{1.19}$$

[14, 1]. For $N \approx Z \approx A/2$ the Fermi energy of each species is

$$\varepsilon_F = \frac{\hbar^2}{2m}(3\pi^2 n)^{2/3} \approx 35\,\mathrm{MeV}, \tag{1.20}$$

corresponding to

$$p_F \approx 265\,\mathrm{MeV}/c, \qquad k_F = p_F/\hbar \approx 1.33\,\mathrm{fm}^{-1}. \tag{1.21}$$

The mean kinetic energy per nucleon in a free Fermi gas is $\frac{3}{5}\varepsilon_F \approx 21\,\mathrm{MeV}$. Neutron-scattering and optical-model analyses place the depth of the mean field near $U \sim -40\,\mathrm{MeV}$; the net volume binding is then of order $a_V \sim |U| - \frac{3}{5}\varepsilon_F \sim 15$–$20\,\mathrm{MeV}$, consistent with the SEMF volume coefficient [14].

These numbers fix the density and energy scales that Lectures 4–6 carry into the liquid-drop formula and into compact-star estimates.

1.9 Deeper reading: from n_0 to SEMF coefficients

Once n_0 and $r_0 = (3/4\pi n_0)^{1/3}$ are fixed, the SEMF volume term a_V is essentially the binding per nucleon in infinite symmetric matter. The surface term a_S measures the energy cost of the diffuse skin of thickness $t \sim 2.3\,\mathrm{fm}$ mapped in Lecture 1. A crude geometric estimate of the surface-to-volume ratio is $3t/R$ for light systems: that is why B/A rises steeply below $A \sim 50$ and flattens thereafter (Lecture 4).

1.9.1 Link to asymmetry and neutron stars

Replacing $N = Z$ by a neutron excess costs the symmetry energy $a_a(N-Z)^2/A$. The density slope of that symmetry energy near n_0 controls both laboratory neutron skins and the pressure of neutron-star matter just above saturation. Thus the pedagogical chain is tight: Lecture 1 measures charge radii, Lecture 2 fixes bulk density, Lecture 4 organises binding, and Lecture 6 asks what happens when gravity compresses the same saturated fluid far beyond n_0.

Keep the bookkeeping honest: quoting n_0 without an uncertainty on the compressibility K or the symmetry slope L understates how many EOS families remain allowed by the same laboratory saturation point.

1.9.2 Saturation as a many-body problem

In modern language, two-nucleon potentials fitted only to scattering underbind or overbind finite nuclei and misplace n_0 unless three-nucleon forces are included at the appropriate chiral order. Students need not master the EFT power counting here, but they should remember that the Fermi-gas estimate of Lecture 2 is a scale argument, not a derivation of the force. Lectures 7–11 rebuild the force from the deuteron upward; Lectures 4–6 spend the saturation scales those forces must reproduce.

A Fermi-gas pressure $P = (2/5)nT_F$ at saturation is tens of mega-electronvolts per cubic femtometre, enormous on laboratory scales yet the baseline that gravity must overcome in Lecture 6. Adding interactions changes both the energy and the pressure; the slope of E/A versus n away from n_0 is the EOS. Students should plot a schematic E/A with a minimum at

n_0 and mark K as curvature: that single sketch organises saturation, giant resonances, and neutron-star radii.

Saturation checklist

Record n_0, $B/A|_{\mathrm{vol}}$, K, and a schematic $S(n)$ slope L whenever you read an EOS paper. Recompute r_0 from your chosen n_0 and verify that $R = r_0 A^{1/3}$ matches Lecture 1 radii at the 5% level for medium-mass nuclei. Discrepancies larger than that usually mean you are mixing charge and matter radii or using a saturated density inconsistent with the SEMF fit of Lecture 4.

From density to pressure

Differentiate a schematic energy per nucleon $E/A = \frac{3}{5}T_F(n) + a(n) + b(n)^2$ to obtain pressure $P = n^2\partial(E/A)/\partial n$. At saturation $P = 0$ by definition; above saturation the same derivative becomes the EOS. Plotting $P(n)$ for two choices of K shows immediately why stellar radii move when incompressibility changes. Keep isoscalar (K) and isovector (L) derivatives distinct in that sketch.

Finite nuclei versus infinite matter

Surface and Coulomb energies vanish in infinite matter but dominate light nuclei. Extracting n_0 from finite nuclei therefore requires a model that removes those corrections. That is why modern determinations combine heavy-nucleus radii, giant resonances, and ab initio infinite-matter calculations rather than reading n_0 from a single A.

Saturation numbers to keep

Memorise four numbers with units: $n_0 \simeq 0.16\,\mathrm{fm}^{-3}$, $B/A \simeq 16\,\mathrm{MeV}$, $K \simeq 240\,\mathrm{MeV}$, and $L \sim 40$–$80\,\mathrm{MeV}$ (broad present range). Every EOS talk rewrites those symbols; students who know the numbers can detect inconsistent plots immediately. Recompute r_0 from n_0 whenever a paper uses a different saturation point, and adjust Lecture 1 radius comparisons accordingly.

Research frontier: saturation, symmetry energy, and student projects

Lecture 2 fixed the saturation density $n_0 \sim 0.16\,\mathrm{fm}^{-3}$ and the volume energy scale from elementary Fermi-gas estimates of kinetic and potential contributions. Those order-of-magnitude arguments still teach why nuclei exist as saturated droplets, but they do not organise the hierarchy of two- and three-nucleon forces. Chiral effective field theory (EFT) now expands residual nuclear interactions systematically in momenta over a breakdown scale, so that saturation and the symmetry energy emerge from low-energy QCD symmetries rather than from a purely phenomenological well [41, 42]. The slope $L = 3n_0(dS/dn)_{n_0}$ of the symmetry energy near n_0 remains one of the most debated nuclear-matter parameters: laboratory skins, heavy-ion collective flow, and neutron-star radii pull in partly different directions, and modern reviews emphasise propagating those uncertainties into astrophysical equations of state [45, 38]. Three-nucleon forces shift the saturation point relative to pure two-nucleon Hamiltonians; omitting them typically misplaces both the binding energy per nucleon and the equilibrium density. Open questions include the size of higher-order chiral truncation errors at twice saturation density and the consistency between terrestrial constraints and multimessenger astrophysics.

A useful way to keep the uncertainty honest is to treat $S(n)$ not as a single curve but as a family of curves consistent with skins, dipole polarizability, and astrophysical radii. Student projects that recompute L from two published parametrisations and then ask which dense-matter observables move the most are closer to current practice than memorising one preferred number.

Student directions. (1) Analytic estimate: convert n_0 between fm^{-3} and $\mathrm{kg\,m}^{-3}$ and rederive $r_0 = (3/4\pi n_0)^{1/3}$. (2) Data project: from a published $S(n)$ parametrisation, extract L and compare with the PREX-implied range. (3) Literature survey: summarise how three-nucleon forces shift the saturation point relative to pure two-nucleon Hamiltonians [41].

1.10 Problems with solutions

Problem 2.1 — Saturation density

Using $R = 1.2\,A^{1/3}\,\mathrm{fm}$, compute the mean nucleon number density $\rho_0 = A/(\frac{4}{3}\pi R^3)$ in fm^{-3} and in $\mathrm{g\,cm}^{-3}$ (take $m_N = 1.67 \times 10^{-24}\,\mathrm{g}$).

Solution 2.1

$$\rho_0 = \frac{3}{4\pi r_0^3} = \frac{3}{4\pi(1.2)^3} \approx 0.138\,\mathrm{fm}^{-3} \sim 0.14\text{–}0.17\,\mathrm{fm}^{-3}$$

depending on the precise radius definition. In mass units,

$$\rho_0 m_N \approx 2.3 \times 10^{14}\,\mathrm{g\,cm}^{-3},$$

as in Problem 1.1. This is the saturation density underlying the SEMF volume term.

Problem 2.2 — Neutron-star radius from density (Petrera 1.1.3)

A neutron star has mass $M \sim M_\odot = 2 \times 10^{30}\,\mathrm{kg}$ and density comparable to nuclear density $\rho \sim 2.3 \times 10^{14}\,\mathrm{g\,cm}^{-3}$. Estimate its radius.

Solution 2.2

$$\frac{4}{3}\pi R^3 \rho = M \quad \Rightarrow \quad R = \left(\frac{3M}{4\pi\rho}\right)^{1/3} \approx \left(\frac{3 \times 2 \times 10^{33}\,\mathrm{g}}{4\pi \times 2.3 \times 10^{14}\,\mathrm{g\,cm}^{-3}}\right)^{1/3} \approx 13\,\mathrm{km}.$$

Nuclear saturation density plus solar mass already yields the observed $R \sim 10\,\mathrm{km}$ scale (Lecture 7).

Problem 2.3 — Surface thickness

For a Woods–Saxon profile with $a = 0.52\,\text{fm}$, compute the skin thickness t over which the density falls from 90% to 10% of its central value.

Solution 2.3

$$t = 4a \ln 3 \approx 4 \times 0.52 \times 1.099 \approx 2.3\,\text{fm}.$$

The surface thickness is nearly independent of A, while $R \propto A^{1/3}$ grows: light nuclei are almost all surface; heavy nuclei have a thin skin on a large bulk.

Bibliography

[1] R. A. Dunlap, *An Introduction to the Physics of Nuclei and Particles* (2nd ed.), IOP Publishing, Bristol (2023), DOI: 10.1088/978-0-7503-6094-4, Ch. 3 (Nuclear composition and size).

[2] W. Demtröder, *Nuclear and Particle Physics*, Undergraduate Lecture Notes in Physics, Springer, Cham (2023).

[3] S. Petrera, *Problems and Solutions in Nuclear and Particle Physics*, UNITEXT for Physics, Springer, Cham (2019).

[4] F. Terranova, *A Modern Primer in Particle and Nuclear Physics*, Oxford University Press (2021).

[5] S. D'Auria, *Introduction to Nuclear and Particle Physics*, Undergraduate Lecture Notes in Physics, Springer, Cham (2018).

[6] K. S. Krane, *Introductory Nuclear Physics*, Wiley, New York (1988).

[7] R. Hofstadter, "Electron scattering and nuclear structure," Rev. Mod. Phys. **28**, 214 (1956).

[8] H. F. Ehrenberg, R. Hofstadter, U. Meyer-Berkhout, D. G. Ravenhall, and S. E. Sobottka, "High-Energy Electron Scattering and the Charge Distribution of Carbon-12 and Oxygen-16," Phys. Rev. **113**, 666 (1959).

[9] H. Yukawa, "On the interaction of elementary particles. I," Proc. Phys.-Math. Soc. Japan **17**, 48 (1935).

[10] R. D. Woods and D. S. Saxon, "Diffuse surface optical model for nucleon-nuclei scattering," Phys. Rev. **95**, 577 (1954).

[11] H. G. J. Moseley, "The high-frequency spectra of the elements," Phil. Mag. **26**, 1024 (1913); **27**, 703 (1914).

[12] C. F. von Weizsäcker, "Zur Theorie der Kernmassen," Z. Phys. **96**, 431 (1935).

[13] P. Cappellaro, *Introduction to Applied Nuclear Physics* (MIT OpenCourseWare / LibreTexts), CC BY-NC-SA 4.0.

[14] J.-L. Basdevant, J. Rich, and M. Spiro, *Fundamentals in Nuclear Physics: From Nuclear Structure to Cosmology*, Springer, New York (2005).

[15] D. Tong, *Particle Physics*, Lecture notes (University of Cambridge / CERN school notes).

[16] M. G. Mayer, "On closed shells in nuclei. II," Phys. Rev. **75**, 1969 (1949).

[17] O. Haxel, J. H. D. Jensen, and H. E. Suess, "On the "magic numbers" in nuclear structure," Phys. Rev. **75**, 1766 (1949).

[18] T. Schmidt, "Über die magnetischen Momente der Atomkerne," Z. Phys. **106**, 358 (1937).

[19] L. W. Nordheim, "On spins, moments, and shells in nuclei," Phys. Rev. **78**, 294 (1950).

[20] Evaluated Nuclear Structure Data File (ENSDF), National Nuclear Data Center, Brookhaven National Laboratory, `https://www.nndc.bnl.gov/ensdf/`.

[21] NuDat 3, National Nuclear Data Center, Brookhaven National Laboratory, `https://www.nndc.bnl.gov/nudat3/`.

[22] N. J. Stone, "Table of nuclear magnetic dipole and electric quadrupole moments," At. Data Nucl. Data Tables **90**, 75 (2005); updated compilations at NNDC.

[23] W. N. Cottingham and D. A. Greenwood, *An Introduction to Nuclear Physics* (2nd ed.), Cambridge University Press, Cambridge (2001).

[24] H. Geiger and J. M. Nuttall, "The ranges of the α particles from the radioactive substances," Phil. Mag. **22**, 613 (1911).

[25] G. Gamow, "Zur Quantentheorie des Atomkernes," Z. Phys. **51**, 204 (1928).

[26] R. W. Gurney and E. U. Condon, "Wave mechanics and radioactive disintegration," Nature **122**, 439 (1928); Phys. Rev. **33**, 127 (1929).

[27] M. Wang, W. J. Huang, F. G. Kondev, G. Audi, and S. Naimi, "The AME 2020 atomic mass evaluation (II). Tables, graphs and references," Chin. Phys. C **45**, 030003 (2021).

[28] Laboratoire National Henri Becquerel (LNHB), Recommended decay data, `http://www.lnhb.fr/nuclear-data/nuclear-data-table/`.

[29] L. M. Langer, R. D. Moffat, and H. C. Price, Jr., "Low energy beta-ray spectra: P^{32} and Cu^{64}," Phys. Rev. **76**, 1725 (1949).

[30] L. M. Langer and H. C. Price, Jr., "Shapes of the beta-spectra of the forbidden transitions of Sb^{124}, Rb^{86}, Sr^{89}, Y^{91}, and Cs^{137}," Phys. Rev. **75**, 1769 (1949).

[31] D. C. Camp and L. M. Langer, "The shape of the ^{66}Ga positron spectrum and the contribution from $0^+ \to 0^+$ transitions," Phys. Rev. **129**, 1782 (1963).

[32] H. C. Verma, *Nuclear Physics: Fundamentals and Applications*, NPTEL/IIT Kanpur lecture series, `https://hcverma.in/ncl_phy_lectures`.

[33] International Atomic Energy Agency, *LiveChart of Nuclides*, evaluated structure, decay, reaction, and fission-yield data, `https://www-nds.iaea.org/relnsd/vcharthtml/VChartHTML.html`.

[34] T. Kibédi, T. W. Burrows, M. B. Trzhaskovskaya, P. M. Davidson, and C. W. Nestor, Jr., "Evaluation of theoretical conversion coefficients using BrIcc," Nucl. Instrum. Methods Phys. Res. A **589**, 202 (2008), DOI: 10.1016/j.nima.2008.02.051.

[35] D. A. Brown *et al.*, "ENDF/B-VIII.0: The 8th major release of the nuclear reaction data library with CIELO-project cross sections, new standards and thermal scattering data," Nucl. Data Sheets **148**, 1 (2018), DOI: 10.1016/j.nds.2018.02.001.

[36] B. Acharya *et al.*, "Solar fusion III: New data and theory for hydrogen-burning stars," Rev. Mod. Phys. **97**, 035002 (2025), DOI: 10.1103/8lm7-gs18.

[37] S. N. Ghoshal, "An experimental verification of the theory of compound nucleus," Phys. Rev. **80**, 939 (1950), DOI: 10.1103/PhysRev.80.939.

[38] D. Adhikari *et al.* (PREX Collaboration), "Accurate determination of the neutron skin thickness of ^{208}Pb through parity-violation in electron scattering," Phys. Rev. Lett. **126**, 172502 (2021), DOI: 10.1103/PhysRevLett.126.172502.

[39] B. T. Reed, F. J. Fattoyev, C. J. Horowitz, and J. Piekarewicz, "Implications of PREX-II on the equation of state of neutron-rich matter," Phys. Rev. Lett. **126**, 172503 (2021), DOI: 10.1103/PhysRevLett.126.172503.

[40] B. Hu *et al.*, "Ab initio predictions link the neutron skin of ^{208}Pb to nuclear forces," Nature Phys. **18**, 1196 (2022), DOI: 10.1038/s41567-022-01715-8.

[41] E. Epelbaum, H.-W. Hammer, and U.-G. Meißner, "Modern theory of nuclear forces," Rev. Mod. Phys. **81**, 1773 (2009), DOI: 10.1103/RevModPhys.81.1773.

[42] H.-W. Hammer, S. König, and U. van Kolck, "Nuclear effective field theory: Status and perspectives," Rev. Mod. Phys. **92**, 025004 (2020), DOI: 10.1103/RevModPhys.92.025004.

[43] T. Otsuka, A. Gade, O. Sorlin, T. Suzuki, and Y. Utsuno, "Evolution of shell structure in exotic nuclei," Rev. Mod. Phys. **92**, 015002 (2020), DOI: 10.1103/RevModPhys.92.015002.

[44] H. Hergert, S. K. Bogner, T. D. Morris, A. Schwenk, and K. Tsukiyama, "The in-medium similarity renormalization group: A novel ab initio method for nuclei," Phys. Rep. **621**, 165 (2016), DOI: 10.1016/j.physrep.2015.12.007.

[45] J. M. Lattimer and M. Prakash, "The equation of state of hot, dense matter and neutron stars," Phys. Rep. **621**, 127 (2016), DOI: 10.1016/j.physrep.2015.12.005.

[46] J. M. Lattimer, "Neutron stars and the nuclear matter equation of state," Annu. Rev. Nucl. Part. Sci. **71**, 433 (2021), DOI: 10.1146/annurev-nucl-102419-124827.

[47] B. P. Abbott *et al.* (LIGO Scientific Collaboration and Virgo Collaboration), "GW170817: Observation of gravitational waves from a binary neutron star inspiral," Phys. Rev. Lett. **119**, 161101 (2017), DOI: 10.1103/PhysRevLett.119.161101.

[48] M. J. Dolinski, A. W. P. Poon, and W. Rodejohann, "Neutrinoless double-beta decay: Status and prospects," Annu. Rev. Nucl. Part. Sci. **69**, 219 (2019), DOI: 10.1146/annurev-nucl-101918-023407.

[49] M. Agostini, G. Benato, J. A. Detwiler, J. Menéndez, and F. Vissani, "Toward the discovery of matter creation with neutrinoless $\beta\beta$ decay," Rev. Mod. Phys. **95**, 025002 (2023), DOI: 10.1103/RevModPhys.95.025002.

[50] P. Gysbers *et al.*, "Discrepancy between experimental and theoretical β-decay rates resolved from first principles," Nature Phys. **15**, 428 (2019), DOI: 10.1038/s41567-019-0450-7.

[51] H. L. Crawford, K. Fossez, S. König, and A. Spyrou, "A vision for the science of rare isotopes," Annu. Rev. Nucl. Part. Sci. **74**, 141 (2024), DOI: 10.1146/annurev-nucl-121423-091501.

[52] Nuclear Science Advisory Committee, *A New Era of Discovery: The 2023 Long Range Plan for Nuclear Science*, U.S. Department of Energy and National Science Foundation (2023), `https://nuclearsciencefuture.org/`.

[53] S. A. Giuliani, Z. Matheson, W. Nazarewicz, E. Olsen, P.-G. Reinhard, J. Sadhukhan, B. Schuetrumpf, N. Schunck, and P. Schwerdtfeger, "Colloquium: Superheavy elements: Oganesson and beyond," Rev. Mod. Phys. **91**, 011001 (2019), DOI: 10.1103/RevModPhys.91.011001.

[54] N. Schunck and D. Regnier, "Theory of nuclear fission," Prog. Part. Nucl. Phys. **125**, 103963 (2022), DOI: 10.1016/j.ppnp.2022.103963.

[55] I. Counts, J. Hur, D. P. L. Aude Craik, H. Jeon, C. Leung, J. C. Berengut, A. Geddes, A. Kawasaki, W. Jhe, and V. Vuletić, "Evidence for nonlinear isotope shift in Yb^+ search for new boson," Phys. Rev. Lett. **125**, 123002 (2020), DOI: 10.1103/PhysRevLett.125.123002.

[56] I. Angeli and K. P. Marinova, "Table of experimental nuclear ground state charge radii: An update," At. Data Nucl. Data Tables **99**, 69 (2013), DOI: 10.1016/j.adt.2011.12.006.

[57] S. Kraemer *et al.*, "Observation of the radiative decay of the ^{229}Th nuclear clock isomer," Nature **617**, 706 (2023), DOI: 10.1038/s41586-023-05894-z.